De 24/06/2026 a 27/06/2026
São Paulo
https://doi.org/10.67775/w9wx9e86

Congresso Brasileiro de Patologia das Construções

# THERMOMECHANICAL RESPONSE OF RC BEAMS UNDER EV FIRE EXPOSURE: A NON-COUPLED CFD–FEA INVESTIGATION

Fabricio L. Bolina[1]*, Débora B. Silva [2]; Eduardo C. Pachla[3]
*Autor de contato: fabriciobolina@gmail.com

[1] Departamento de Engenharia Civil, Universidade Federal do Rio Grande do Sul, Porto Alegre, Brasil
[2] Departamento de Arquitetura, Universidade Federal de Santa Maria, Santa Maria, Brasil
[3] Departamento de Estruturas e Construção Civil, Universidade Federal de Santa Maria, Santa Maria, Brasil

**ABSTRACT**

This study evaluates the thermomechanical response of reinforced concrete (RC) beams subjected to Electric Vehicles (EV) fire scenarios, which impose more severe thermal loads than the ISO 834 curve adopted in EN 1992-1-2. A coupled thermal–mechanical finite element analysis (FEA) was conducted on nine beams, varying reinforcement layout, diameter, and concrete cover thickness. Compared with code-based predictions, EV fires reduced fire resistance by up to 27% within 60 min. Increasing concrete cover (≥30 mm) and using multiple reinforcement layers improved performance by limiting steel stresses. Results suggest current provisions may underestimate EV fire, indicating the need to update fire resistance criteria and detailing rules for RC structures.
*Palavras-chave: beam; reinforced concrete; structures in fire; electric vehicles.*

**RESUMO**

Este estudo avaliou a resposta termomecânica de vigas de concreto armado submetidas a cenários de incêndio envolvendo veículos elétricos (VE), os quais impuseram solicitações térmicas mais severas do que a curva ISO 834 adotada na EN 1992-1-2. Foi realizada uma análise numérica termomecânica por elementos finitos em nove vigas, variando-se o arranjo das armaduras, o diâmetro das armaduras e a espessura do cobrimento destas. Em comparação com as previsões baseadas em normas, os incêndios de VE reduziram o tempo de resistência ao fogo em até 27% nos primeiros 60 min. O aumento do cobrimento (≥ 30 mm) e a adoção de múltiplas camadas de armadura melhoraram o desempenho, ao limitar os níveis de tensão no aço. Os resultados indicam que as normas atuais podem subestimar as demandas impostas por incêndios de VE, evidenciando a necessidade de revisão dos critérios de resistência ao fogo e das regras de detalhamento para estruturas de concreto armado.
*Keywords: vigas; concreto armado; estruturas ao incêndio; veículos elétricos.*

## 1. INTRODUCTION

O Climate change and interest to reduce the total $CO_2$ emissions have driven demand for cleaner technologies, making electric vehicles (EVs) a key part of sustainable mobility. In 2023, EVs accounted for 18% of global vehicle sales (up from 14% in 2022 and just 2% in 2018) with over 14 million units sold, 3.5 million more than the previous year. Weekly registrations peaked at 250,000, surpassing the total sales recorded in 2013. (IEA, 2024). This rapid increase is driven by the application of lithium-ion batteries (LIBs) (Wu *et al.*, 2018).

EV fires present distinct hazards: high heat release, toxic gas emission (e.g., HF), explosion risk, re-ignition potential, and prolonged, water-intensive suppression. These risks are amplified in confined spaces, posing significant challenges to fire safety engineering and EV deployment. (Funk *et al.*, 2023; Internal Association of Fire, 2022; Mier *et al.*, 2017; Sturm *et al.*, 2022).

Thermal runaway in LIB batteries can be triggered by improper use, abusive conditions such as overheating, overcharging, short circuits, or mechanical impact (Sun *et al.*, 2020), or exposure to extreme factors. These events initiate exothermic reactions that release heat, flammable gases, and toxic byproducts, potentially resulting in fires or explosions (Li *et al.*, 2019; Peng *et al.*, 2020). EV fires have also occurred during stationary charging. As a result, EV fires in enclosed spaces pose heightened risks to RC structures due to limited ventilation and restricted firefighting access (Funk *et al.*, 2023).

Kang et al. (Kang *et al.*, 2023) conducted large-scale LIB fire tests, showing that EV fires can last up to 70 min and exceed the thermal severity of the ISO 834 adopted in EN 1992-1-2. Structural behavior was not assessed, reinforcing the need to evaluate EV fire effects on structural integrity. The studies in enclosed environments (Kang *et al.*, 2023; Sturm *et al.*, 2020, 2022), primarily assess thermal parameters and toxic gas emissions. However, focus solely on fire dynamics and neglect the compartment temperature development and its structural implications. No study evaluates the structural performance of RC elements exposed to EV fire. This gap underscores the novelty of the present study, which addresses the structural response of RC members under EV fire.

Sturm et al. (Sturm *et al.*, 2022) performed full-scale EV fire tests in a road tunnel. EVs showed higher heat release rates, and hydrogen fluoride was identified as a critical byproduct. Although different firefighting methods were evaluated, the study did not assess structural temperatures or fire impact on structural performance: an aspect addressed in the present research.

Funk et al. (Funk *et al.*, 2023) conducted nine EV fire tests in an open-sided enclosure, recording gas and ceiling temperatures up to 1000 °C and fire spread to adjacent vehicles within 3–46 min. Although no structural analysis of RC elements was performed, the results indicated significant risks to structural integrity, reinforcing the need for research on RC performance under EV fire.

Fires in residential buildings cause significant fatalities, damage, and economic losses (Bolina *et al.*, 2020; Dundar and Selamet, 2023), with high-rises especially vulnerable due to their complexity and evacuation challenges. However, EV fires raise additional concerns. Elevated temperatures degrade concrete and steel, risking structural failure and collapse. Current RC design standards, such as EN 1992-1-2 (EN 1992-1.2, 2004) and NBR 15200 (NBR 15200, 2024), rely on ISO 834 (ISO 834, 1999) but EV fires can exceed this severity, leaving the adequacy of existing codes for EV fire scenarios unverified.

This study addresses a key gap in structural fire safety related to sustainability. EV fires may exceed ISO 834 temperatures within 45–60 min, challenging the assumptions of EN 1992-1-2. As RC degradation is temperature-dependent, it is crucial to verify whether code-designed elements maintain adequate safety under these intensified thermal demands, particularly in basements, where beams are exposed on three sides and EV parking increases the risk of fire-induced damage, progressive collapse, and reduced structural resilience.

Three RC beams with equal flexural capacity at ambient temperature but different reinforcement layouts and rebar diameters were modeled. Coupled thermomechanical FEA was performed under ISO 834 and EV curves, with beams loaded to 70% of their room-temperature ultimate capacity. As all met the 60-min criterion, six additional beams representing critical conditions (reduced cover, lower reinforcement, higher load levels) were analyzed, totaling nine cases. The objective is to verify whether EN 1992-1-2 provisions adequately ensure RC performance under EV fires or require revision for this intensified hazard.

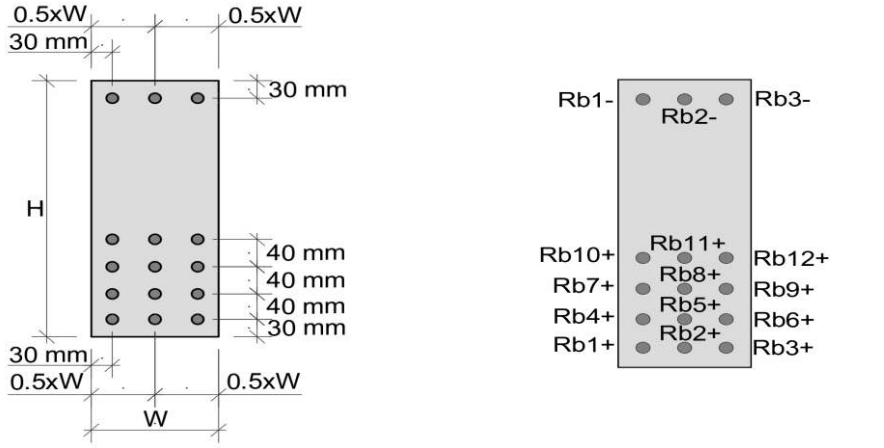
## 2. METHODS

The study was conducted in three stages: (i) development of RC beam models with identical cross-sections but varying reinforcement layouts, rebar diameters, and concrete cover thickness- ensuring equivalent ultimate capacity while also simulating critical conditions (e.g., low reinforcement ratios and reduced cover typical of older, noncompliant structures); (ii) thermal FEA to obtain cross-sectional temperature fields under ISO 834 and an EV-specific fire curve derived from CFD and experimental data; and (iii) coupled thermomechanical FEA applying these temperature fields to beams subjected to 70% of their ultimate load or to critical load levels, enabling comparison of ISO and EV fire impacts in terms of reinforcement yielding, stiffness degradation, and deflection.

### 2.1 Beam cases

The beam cross-sectional geometry and corresponding reinforcement layout are shown in Figure 1. All models share a width (W) of 200 mm and a total height (H) of 600 mm, with 6,000 mm in span. The reinforcement layouts, concrete cover values, and the conventions are shown in Table 1.

Figure 1 – Steel reinforcement distributed across the beam cross section




(a) Reinforcements arrangement (b) Reinforcements nomenclature

Table 1 – Beam cases based on reinforcement diameter and cross-sectional reinforcement layout

| RC beams naming convention | Reinforcements (steel rebars) | | | | | | | | | | | | | | | |
|---|---|---|---|---|---|---|---|---|---|---|---|---|---|---|---|---|
| | Tensile (positive) | | | | | | | | | | | | Compressive (negative) | | | Concrete cover (mm) |
| | Rb1+ | Rb2+ | Rb3+ | Rb4+ | Rb5+ | Rb6+ | Rb7+ | Rb8+ | Rb9+ | Rb10+ | Rb11+ | Rb12+ | Rb1- | Rb2- | Rb3- | |
| Condition 1: with mechanical equivalence (real load condition) | | | | | | | | | | | | | | | | |
| B1-D10-C20 | 10.0 | 10.0 | 10.0 | 10.0 | 10.0 | 10.0 | 10.0 | 10.0 | 10.0 | 10.0 | 10.0 | 10.0 | 10.0 | 10.0 | 10.0 | 20 |
| B2-D12-C20 | 12.5 | 12.5 | 12.5 | 12.5 | 12.5 | 12.5 | 12.5 | — | — | — | — | — | 10.0 | 10.0 | 10.0 | 20 |
| B3-D16-C20 | 16.0 | 16.0 | 16.0 | 16.0 | — | 16.0 | — | — | — | — | — | — | 10.0 | 10.0 | 10.0 | 20 |
| Condition 2: with no mechanical equivalence (critical load condition with low reinforcement ratio) | | | | | | | | | | | | | | | | |
| B4-D8-C20 | 8.0 | 8.0 | 8.0 | — | — | — | — | — | — | — | — | — | 8.0 | — | 8.0 | 20 |
| B5-D8-C20 | 8.0 | — | 8.0 | — | — | — | — | — | — | — | — | — | 8.0 | — | 8.0 | 20 |
| B6-D10-C20 | 10.0 | — | 10.0 | — | — | — | — | — | — | — | — | — | 10.0 | — | 10.0 | 20 |
| Condition 3: with no mechanical equivalence (critical load condition with different concrete cover thickness) | | | | | | | | | | | | | | | | |
| B7-D10-C10 | 10.0 | — | 10.0 | — | — | — | — | — | — | — | — | — | 10.0 | — | 10.0 | 10 |
| B8-D10-C15 | 10.0 | — | 10.0 | — | — | — | — | — | — | — | — | — | 10.0 | — | 10.0 | 15 |
| B9-D10-C30 | 10.0 | — | 10.0 | — | — | — | — | — | — | — | — | — | 10.0 | — | 10.0 | 30 |

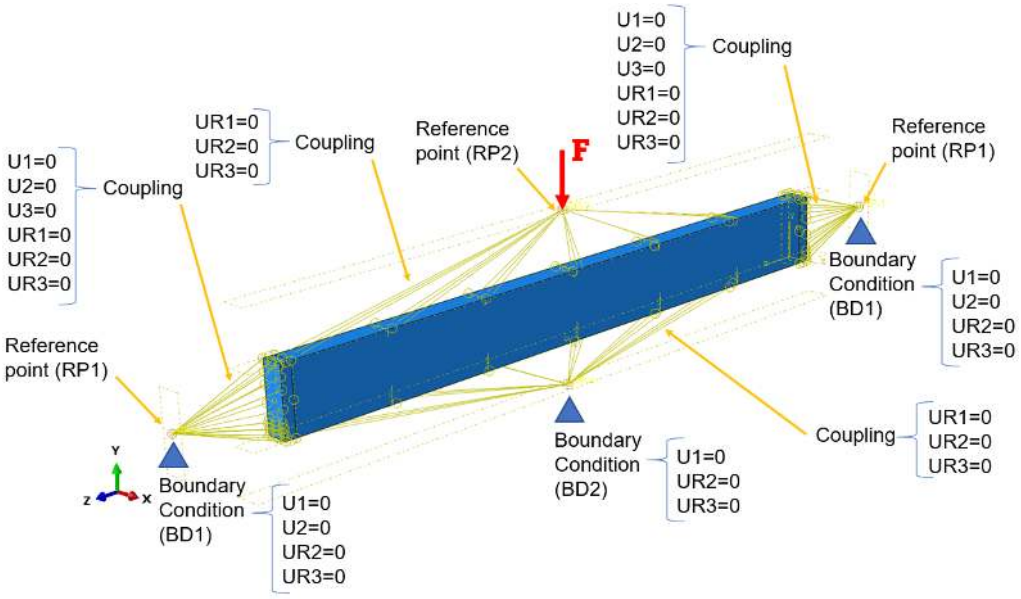
The RC beams have 30 mm vertical and 70 mm horizontal spacing between reinforcement layers. In Condition 1, specimens B1 (Ø10), B2 (Ø12.5), and B3 (Ø16) use 20 mm concrete cover and 500 MPa steel, with equivalent bending capacity but different reinforcement layouts—B3 reflecting typical code-compliant detailing, and B1–B2 using more rebars of smaller diameter to achieve the same strength. As 60 minutes of fire resistance is generally acceptable, two additional non-standard scenarios were examined: Condition 2 includes beams with a reduced number of longitudinal rebars in a single layer (Ø8 and Ø10), simulating older (non-standardized) structures; Condition 3 adds reduced concrete cover (10–15 mm) to represent deficient fire and durability design, with one high-cover beam (30 mm) as reference.

## 2.2 FEA model

a) Mechanical

The RC beam was modeled using nonlinear FEA (Figure 2). Concrete was represented by 3D solid elements and longitudinal reinforcement by truss elements, assuming perfect bond via embedded constraints to ensure full strain compatibility. Nodes included three translational and three rotational degrees of freedom, enabling bending and torsion simulation. A mesh sensitivity analysis (5–30 mm) showed that sizes finer than 20 mm yielded negligible differences in global response, while coarser meshes affected peak load; thus, a 10 mm mesh was adopted.

Figure 2 – Mechanical FE model of RC beams at ambient temperature

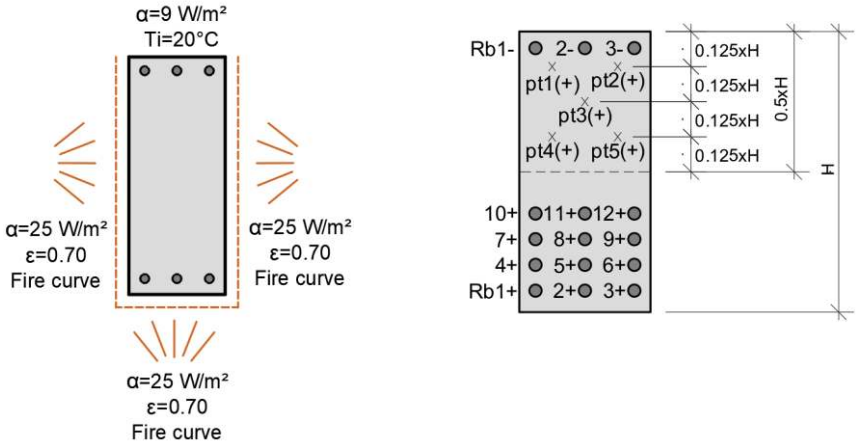



The ultimate bending capacity was obtained by applying a time-dependent load equal to $F$=100.$t$ (N), where "t" is time in s, uniformly distributed on the beam's top surface via a coupling constraint to ensure consistent force transfer. Concrete behavior was modeled using the Concrete Damage Plasticity Model (CDPM) parameters: see the CDPM parameters in (Bolina, 2025).

b) Thermal

The termal FEA model and selected control points (Figure 3) capture temperature evolution in the compressed concrete zone and at reinforcement levels (pt1+ to pt5+); although all rebar layers are illustrated, not all configurations include multiple layers.

Figure 3 – Fire-exposed sides and control points in the beam cross-section




(a) Sides exposed to fire (b) Control points (temperature)

A FEA thermal analysis was performed to determine the time-dependent temperature fields across the beam cross-section under two fire scenarios: ISO 834 and an EV fire. Temperature-dependent thermal properties of concrete and steel were defined according to EN 1992-1-2.

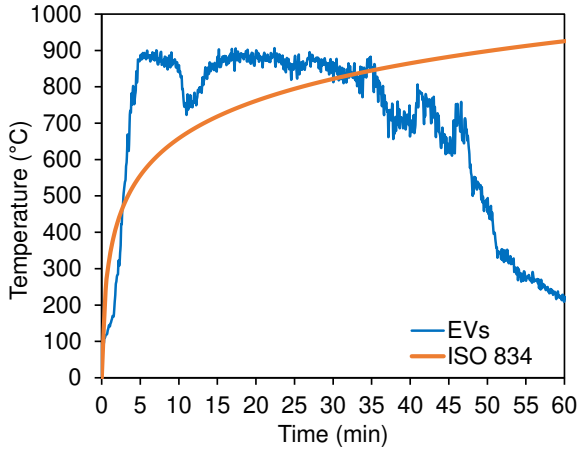
c) Thermo-Mechanical

Cross-sectional temperature fields from the thermal analysis were applied to the mechanical model to account for temperature-induced material degradation, with strength and stiffness reductions defined by EN 1992-1-2 (concrete) and EN 1993-1-2 (steel). The coupled thermomechanical approach enables direct comparison of ISO 834 and EV fire, particularly on bending capacity, using consistent stress and deflection control parameters throughout the simulations.

### 2.3 CFD model

The standardized fire defined by (ISO 834, 1999) is widely recognized and adopted by EN 1992-1-2 (EN 1992-1.2, 2004). In contrast, the EV fire used in this study was previously developed and published by the authors: see (Bolina *et al.*, 2025). The EV fire curve was established using a computational fluid dynamics (CFD) model, which incorporated heat release parameters obtained from experimental studies available in the literature (Kang *et al.*, 2023). The CFD model was validated by full-scale experimental data also extracted from published research (K. Sharma *et al.*, 2021; McGrattan, 2006). The resulting EV fire is shown in Figure 4.

Figure 4 – Standardized fire curve versus the EV fire curve

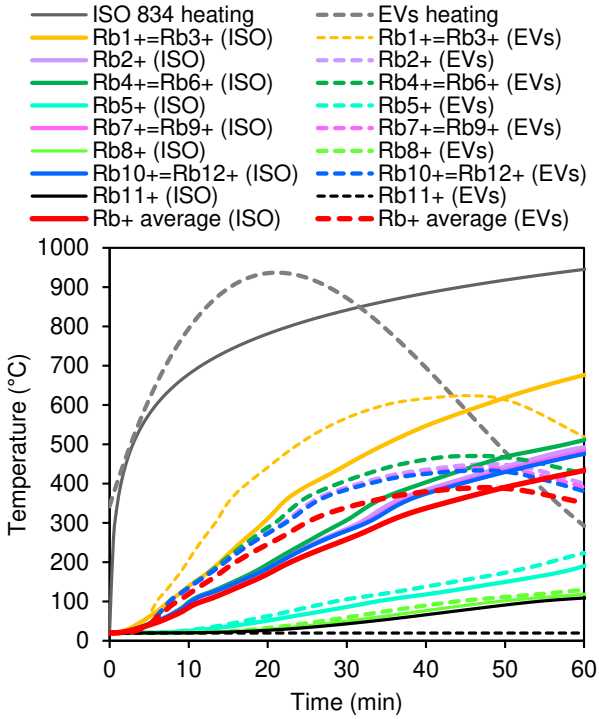



Between 3 and 35 min, EV fire temperatures markedly exceed the ISO 834 curve, highlighting the need to reassess RC fire performance under more severe early-stage heating. The EV curve used herein was previously developed by the authors from CFD simulations calibrated with full-scale EV fire tests and literature data. It represents a single-vehicle fire in a confined, low-ventilation environment (e.g., underground parking), with rapid heating to peak gas temperatures above 1100–1200 °C within 15–25 minutes, followed by decay.

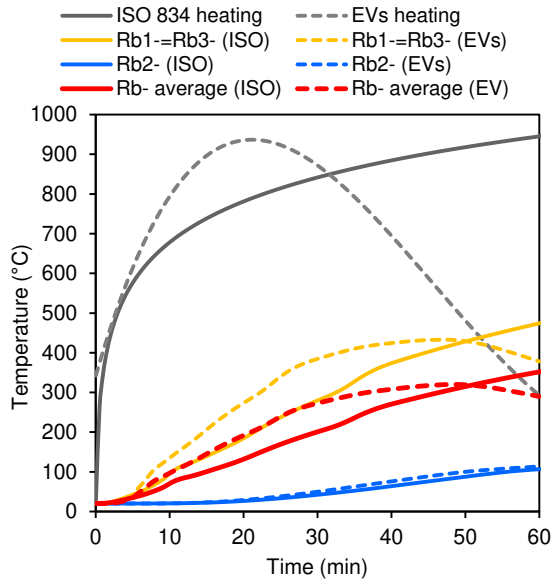
## 3. RESULTS

Figure 5 describes the temperature evolution in the reinforcement, as well as in the concrete above the neutral axis.

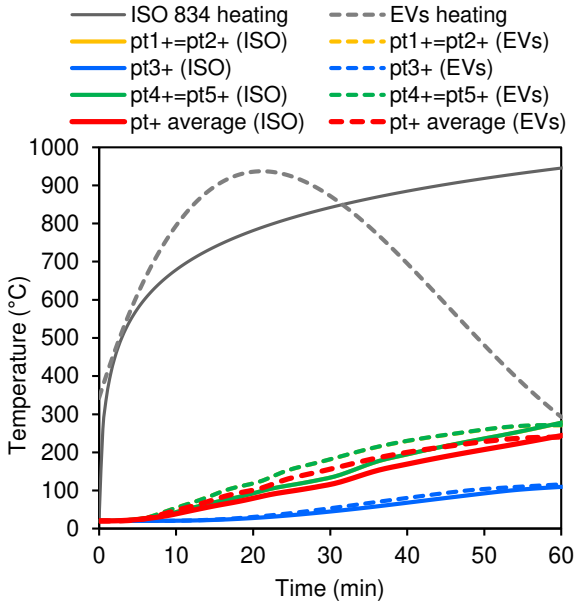
Figure 5 – Temperature history in the beams cross-section




(a) Tensile rebars (Rb1+ to Rb12+)




(b) Compressive rebars (Rb1- to Rb3-)




(c) Concrete control points above the neutral axis (pt1 to pt5)

Corner reinfocercements are more vulnerable to fire due to their proximity to exposed surfaces, which accelerates heat uptake and early strength loss, whereas centrally embedded reinforcements benefit from greater thermal inertia. Denser or more internally distributed reinforcement improves thermal shielding and redundancy. Reinforcement above the neutral axis is particularly susceptible, as steel's high conductivity and low heat capacity intensify temperature rise, making steel degradation the primary driver of fire-induced capacity loss. Under the EV curve, steeper thermal gradients accelerate reinforcement deterioration and reduce bending resistance more rapidly than ISO 834. In the first 45 minutes, average concrete temperatures above the neutral axis under EV

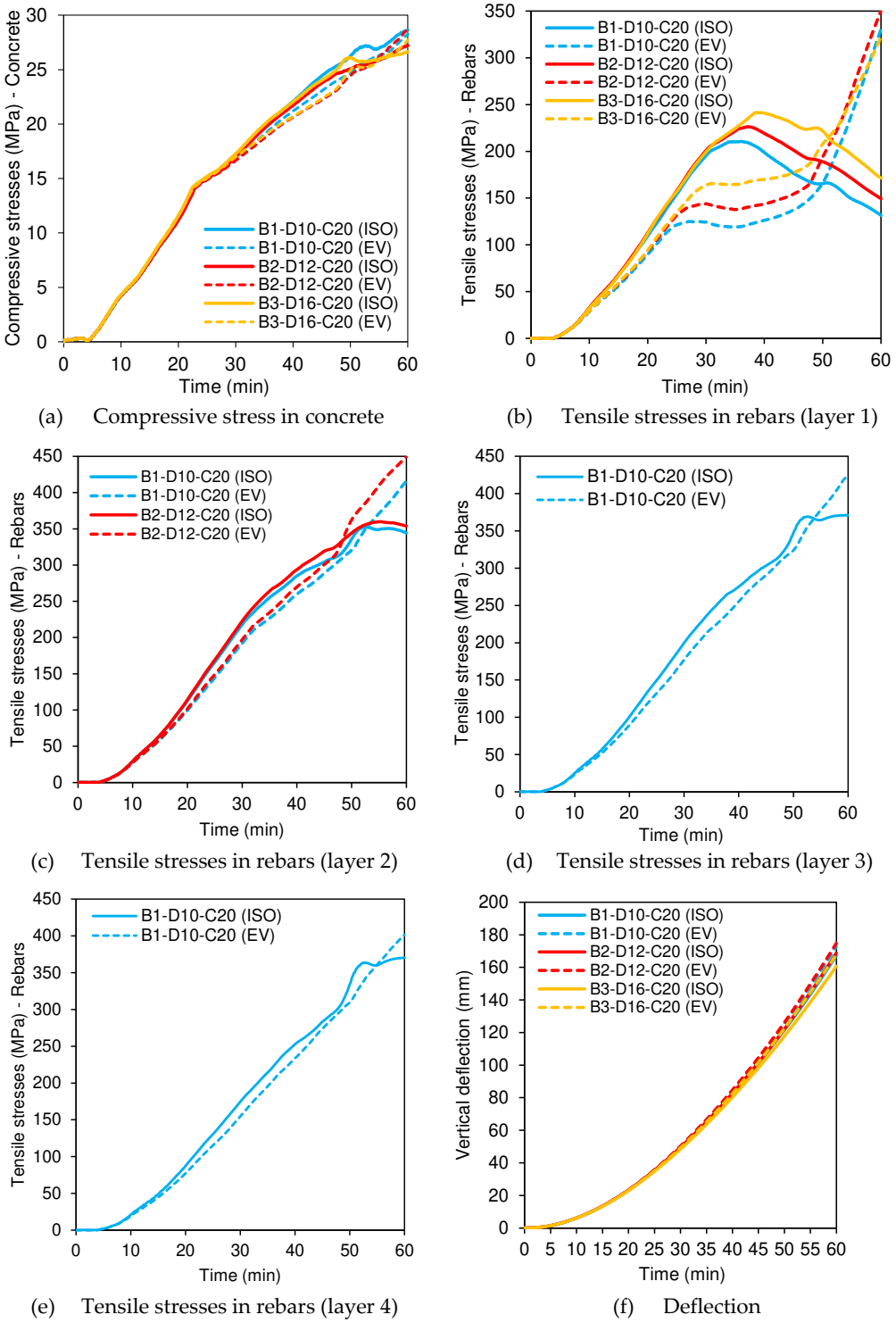
fire were 9.5%, 30.2%, and 12.5% higher than ISO at 15, 30, and 45 min, respectively; positive reinforcement temperatures were 51.4%, 28.2%, and 5.7% higher.

### 3.1 Ultimate load at high temperatures

a) Condition 1

Condition 1 results are shown in Figure 6.

Figure 6 – Tensions and deflections in the beams B1 to B3 – Condition




(a) Compressive stress in concrete

(b) Tensile stresses in rebars (layer 1)

(c) Tensile stresses in rebars (layer 2)

(d) Tensile stresses in rebars (layer 3)

(e) Tensile stresses in rebars (layer 4)

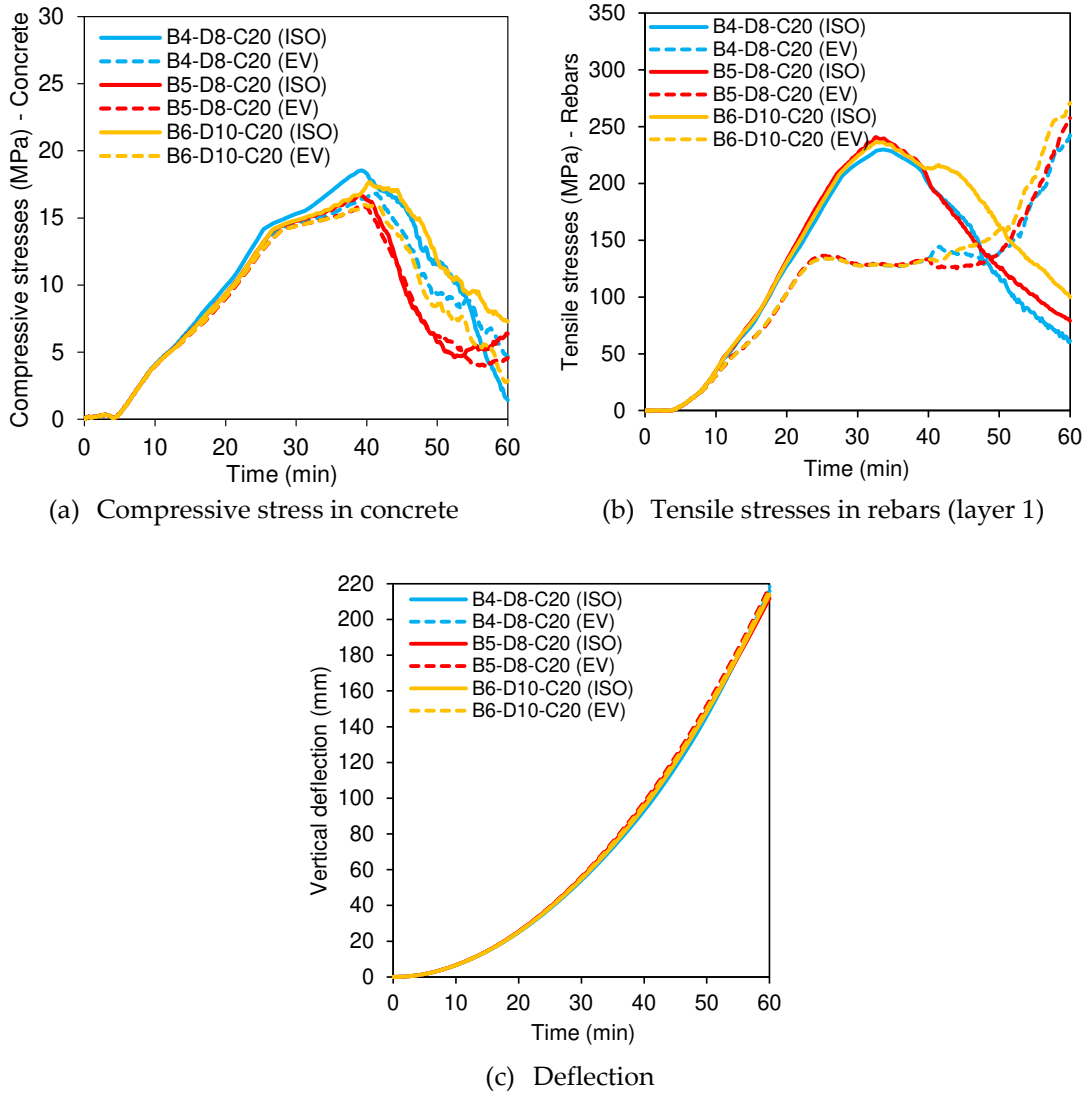
(f) Deflection

Under a sustained load of 70% of ambient ultimate capacity, all RC beams maintained structural stability for 60 minutes under both EV and ISO 834 fires, with no collapse observed (see Figure 6). Although the outer reinforcement layer yielded, concrete compression and stresses in the inner reinforcement layers remained below critical limits, enabling effective stress redistribution and preservation of residual bending capacity. Yielding of the first layer occurred significantly earlier under EV fire (22–27 min) than under ISO fire (30–37 min), corresponding to an approximately 27% reduction in time to yielding; smaller-diameter bars exhibited faster thermal response. Differences in rebar stresses (≤1 MPa) and concrete compression (≤2 MPa) between fire scenarios were modest. None of the beams approached the EN 1363-1 deflection limit (L/20), confirming that thermally induced material degradation (rather than excessive midspan deflection) governed structural performance within the evaluated period (Bolina *et al.*, 2023).

b) Condition 2

Condition 2 results are shown in Figure 7.

Figure 7 – Tensions and deflections in the beams B4 to B6 – Condition 2




(a) Compressive stress in concrete

(b) Tensile stresses in rebars (layer 1)

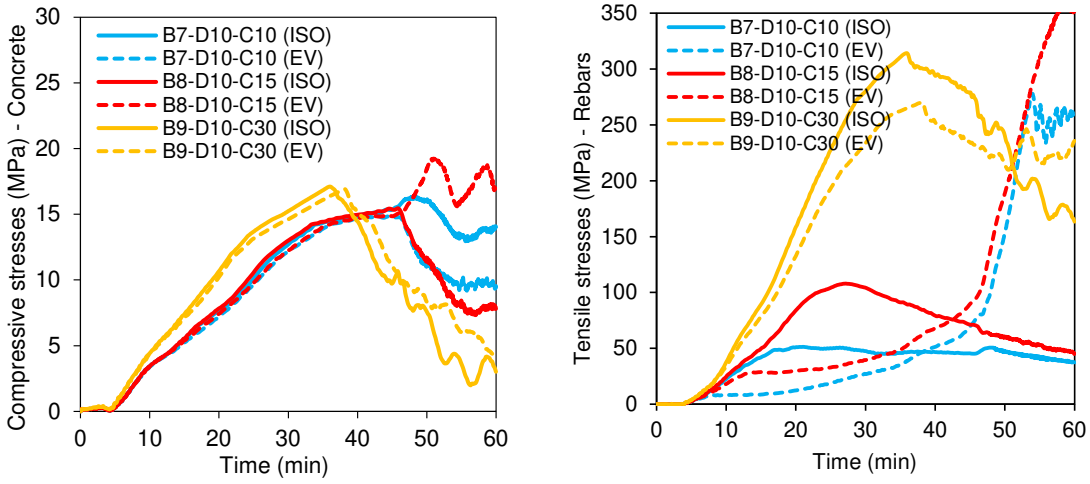
(c) Deflection

This condition examines beams with a single reinforcement layer, 20 mm cover, and high load ratio (as in B1–B3). Owing to the lack of redundancy, both steel and concrete reached yielding earlier than in multi-layer configurations. Reinforcement yielding occurred before 30 minutes under both ISO 834 and EV fires, with EV exposure leading to yielding approximately 9 minutes earlier, confirming its greater thermal severity. The outer (perimetral) rebars were the most vulnerable due to rapid temperature rise and accelerated steel strength degradation. In beam B4, intermediate longitudinal reinforcement provided only marginal delay in thermal penetration and stress redistribution, indicating that single-layer, low-reinforcement layouts lack sufficient thermal inertia and internal redundancy, resulting in a more brittle response. Despite this, beams B4 and B6 did not exceed the EN 1363-1 deflection limit, showing that although stiffness and strength were significantly reduced, deformation capacity remained within acceptable bounds; thus, both resistance and serviceability criteria are essential in fire design. Results re shown in Figure 7.

c) Condition 3

As shown in Figure 8, reducing concrete cover to 10–15 mm markedly accelerates failure under EV fire, as the diminished insulation allows rapid heat transfer to the outer rebars during the intense initial phase (peak within ~15 min). Consequently, steel temperatures rise faster, leading to earlier mechanical degradation and rebar yielding—about 10–12 minutes sooner than under ISO 834. In contrast, with cover ≥30 mm, reinforcement temperatures remain below critical thresholds during the most severe 30–45 minutes of EV exposure. The low thermal diffusivity of concrete delays heat penetration, and because EV fires exhibit a sharp peak followed by early decay, the duration of extreme heating is limited. Under these conditions, beams subjected to EV and ISO fires show similar times to failure, indicating that increased cover effectively mitigates the higher thermal severity of EV scenarios. Thus, adequate concrete cover acts as a robust passive protection measure, particularly for short-duration, high-intensity EV fires.

Figure 8 – Tensions in the beams B7 to B9 – Condition 3




(a) Compressive stress in concrete

(b) Tensile stresses in rebars (layer 1)

## 4. CONCLUSION

This study evaluated the thermomechanical performance of RC beams under EV fire and compared results with ISO 834 predictions. The main conclusions are:

- EV fires generate more critical heating, especially within the first 30–45 min, potentially exceeding the thermal demand assumed in current code-based design.

- Faster temperature rise under EV exposure reduced time to reinforcement yielding by up to ~27%, primarily affecting outer (perimetral) rebars.

- Beams with multiple reinforcement layers maintained integrity through stress redistribution, whereas single-layer configurations showed significantly greater vulnerability.

- Increasing cover to ≥30 mm enhanced thermal insulation, delayed steel degradation, and improved structural resilience, demonstrating its relevance beyond durability considerations.

- Structural response was governed by material strength degradation rather than deflection, as no beam exceeded prescribed deformation limits.

In general, reliance solely on ISO 834 may underestimate the structural demand imposed by EV fires. The findings indicate the need to reassess fire design assumptions, reinforcement detailing, and minimum cover requirements in EV-prone environments, particularly enclosed parking areas, supported by further experimental and system-level research.

## REFERENCES

Bolina, F.L. (2025), *Modelagem Computacional de Estruturas de Concreto Armado Em Elementos Finitos*, edited by Sorian, 1st ed., Vol. 1, Araucária, Paraná.

Bolina, F.L., Fachinelli, E.G. and Rodrigues, J.P.C. (2025), "Analysis of building structures subjected to electric vehicle fires", *Journal of Building Engineering*, Vol. 107, p. 112769, doi: https://doi.org/10.1016/j.jobe.2025.112769.

Bolina, F.L., Gil, A.M., Fernandes, B., Hennemann, G.G., Gonçalves, J. and Tutikian, B.F. (2020), "Influence of design durability on concrete columns fire performance", *Journal of Materials Research and Technology*, Vol. 9 No. 3, pp. 4968–4977, doi: https://doi.org/10.1016/j.jmrt.2020.03.015.

Bolina, F.L., Schallenberger, M. and Carvalho, H. (2023), "Experimental and numerical evaluation of RC ribbed slabs in fire conditions", *Structures*, Vol. 51, pp. 747–759, doi: https://doi.org/10.1016/j.istruc.2023.03.057.

Dundar, U. and Selamet, S. (2023), "Fire load and fire growth characteristics in modern high-rise buildings", *Fire Safety Journal*, Vol. 135, p. 103710, doi: https://doi.org/10.1016/j.firesaf.2022.103710.

EN 1992-1.2. (2004), "Eurocode 2: Design of concrete structures - Part 1-2: General rules - Structural fire design", *European Committee for Standardization*, European Standard, Brussels, Belgium.

Funk, E., Flecknoe-Brown, K.W., Wijesekere, T., Husted, B.P. and Andres, B. (2023), "Fire extinguishment tests of electric vehicles in an open sided enclosure", *Fire Safety Journal*, Vol. 141, p. 103920, doi: https://doi.org/10.1016/j.firesaf.2023.103920.

IEA. (2024), "Global EV Outlook 2024", available at: https://www.iea.org/reports/global-ev-outlook-2024 (accessed 21 September 2024).

Internal Association of Fire. (2022), “Up to 150 000 liters of water needed to put out a fire in an electric car”, available at: https://www.ctif.org/news/150-000-liters-water-needed-put-out-fire-electric-car (accessed 21 September 2024).

ISO 834. (1999), “Fire-resistance tests — Elements of building construction — Part 1: General requirements”, *International Organization for Standardization*, Geneva.

K. Sharma, P., Gera, B. and Singh, R.K. (2021), “A CFD Validation of Fire Dynamics Simulator for Corner Fire”, *CFD Letters*, Vol. 2 No. 4, pp. 137–148.

Kang, S., Kwon, M., Yoon Choi, J. and Choi, S. (2023), “Full-scale fire testing of battery electric vehicles”, *Applied Energy*, Vol. 332, p. 120497, doi: https://doi.org/10.1016/j.apenergy.2022.120497.

Li, H., Duan, Q., Zhao, C., Huang, Z. and Wang, Q. (2019), “Experimental investigation on the thermal runaway and its propagation in the large format battery module with Li(Ni1/3Co1/3Mn1/3)O2 as cathode”, *Journal of Hazardous Materials*, Vol. 375, pp. 241–254, doi: https://doi.org/10.1016/j.jhazmat.2019.03.116.

McGrattan, K. (2006), “Fire Dynamics Simulator (Version 4) Technical Reference Guide”, *NIST Special Publication 1018*, pp. 1–116.

Mier, F.A., Morales, R., Coultas-McKenney, C.A., Hargather, M.J. and Ostanek, J. (2017), “Overcharge and thermal destructive testing of lithium metal oxide and lithium metal phosphate batteries incorporating optical diagnostics”, *Journal of Energy Storage*, Vol. 13, pp. 378–386, doi: https://doi.org/10.1016/j.est.2017.08.003.

NBR 15200. (2024), “Design of reinforced concrete structures in case of fire (in Portuguese)”, *Brazilian National Standards Organization*, Brazilian Standard Association, Rio de Janeiro, Brazil.

Peng, Y., Yang, L., Ju, X., Liao, B., Ye, K., Li, L., Cao, B., *et al.* (2020), “A comprehensive investigation on the thermal and toxic hazards of large format lithium-ion batteries with LiFePO4 cathode”, *Journal of Hazardous Materials*, Vol. 381, p. 120916, doi: https://doi.org/10.1016/j.jhazmat.2019.120916.

Sturm, P., Fößleitner, P., Fruhwirt, D., Galler, R., Wenighofer, R., Heindl, S.F., Krausbar, S., *et al.* (2022), “Fire tests with lithium-ion battery electric vehicles in road tunnels”, *Fire Safety Journal*, Vol. 134, p. 103695, doi: https://doi.org/10.1016/j.firesaf.2022.103695.

Sturm, P., Fössleitner, P., Fruhwirt, D., Schirmer, A., Reinwald, B., Kühbacher, M., Wenighofer, R., *et al.* (2020), “Brandversuch mit E-Fahrzeugen in Tunnelanlagen”, *BHM Berg- Und Hüttenmännische Monatshefte*, Vol. 165 No. 12, pp. 651–657, doi: 10.1007/s00501-020-01054-2.

Sun, P., Bisschop, R., Niu, H. and Huang, X. (2020), “A Review of Battery Fires in Electric Vehicles”, *Fire Technology*, Vol. 56 No. 4, pp. 1361–1410, doi: 10.1007/s10694-019-00944-3.

Wu, T., Chen, H., Wang, Q. and Sun, J. (2018), “Comparison analysis on the thermal runaway of lithium-ion battery under two heating modes”, *Journal of Hazardous Materials*, Vol. 344, pp. 733–741, doi: https://doi.org/10.1016/j.jhazmat.2017.11.022.